CONF-9705143--2

LA-UR-97- 1867

Title: AUGER PARAMETER DETERMINATION OF BONDING STATES ON THINLY OXIDIZED SILICON NITRIDE

Author(s): THOMAS N. TAYLOR, MST-6
DARRYL P. BUTT, MST-6
CARLO G. PANTANO, PENN STATE UNIVERSITY

Submitted to: SURFACE ANALYSIS '97 AND 33RD ANNUAL SYMPOSIUM OF THE NM CHAPTER OF THE AVS IN ALBUQUERQUE, NM ON MAY 20-22, 1997

DISCLAIMER

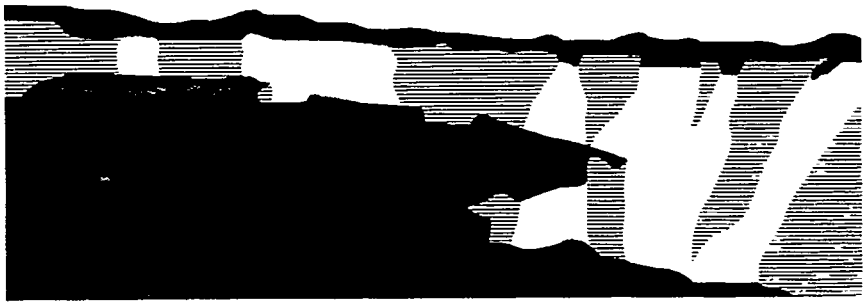

Los Alamos
NATIONAL LABORATORY

Form No. 836 R5
ST 2629 10/91

AUGER PARAMETER DETERMINATION OF BONDING STATES ON THINLY OXIDIZED SILICON NITRIDE

T. N. Taylor and D. P. Butt
Materials Science and Technology : Metallurgy
Los Alamos National Laboratory, Los Alamos, NM 87545

C. G. Pantano
Department of Materials Science and Engineering
Pennsylvania State University, University Park, PA 16802

Silicon nitride powders have been thermally oxidized between 700 and 1200°C in a high purity N_2 - 20% O_2 gas environment. The powders were subsequently analyzed by x-ray photoelectron and Auger electron spectroscopy for evidence of oxynitride surface states. Measurements were made on the Si 2p, O 1s, N 1s, C 1s, F 1s, and Si KLL transitions, the latter being obtained using bremsstrahlung radiation from the Mg x-ray source. As a function of increasing temperature the data show a clear progression of spectral binding energies and peak shapes that are indicative of more advanced surface oxidation. However, definitive analysis of these data rests on the combined use of both Auger and photoelectron data to define the oxidized surface states for a system that involves two electrically insulating end states, silicon nitride and silicon dioxide. Curve fitting the Si 2p and Si KLL transitions as a function of oxidation, coupled with use of Auger parameters for the starting silicon nitride and final silicon dioxide, reveals no measurable evidence for an interphase oxynitride in the thin oxide scales of this study, where the silicon nitride substrate is detectable. Possible incorrect assignment of oxynitride bonding, from shifted Si 2p states in the carbon referenced spectra, is attributable to band bending as the transition is made from incipient to fully formed silicon dioxide.

I. INTRODUCTION

The kinetic and atomic-level processes involved in the thermal oxidation of Si_3N_4 have been the subject of numerous studies [1]. A major focus of these efforts has been verification of an interphase oxynitride that exists between the Si_3N_4 substrate and the outermost SiO_2 coating. The character of this interphase has been a subject of vigorous debate because of the implication that it has for modeling and understanding the fundamental dynamics of the oxidation process [2,3]. For atmospheric oxidation studies of Si_3N_4 below 1200°C, where the oxide is tens of angstroms thick, surface analysis has been used to find evidence of a Si bonding configuration that is intermediate between Si_3N_4 and SiO_2. In some instances these studies have been interpreted to give evidence of an oxynitride [4-6]. Higher temperatures and more advanced oxidation have been found to thicken the interphase region, making it more accessible for study by less surface-sensitive probes, such as ion-scattering spectroscopy and index of refraction measurements. These measurements have been interpreted to show either a graded oxynitride [2] or a distinct Si_2N_2O compound [7], the latter being predicted by the Si-N-O phase equilibrium diagram.

In the current study we have used x-ray photoelectron spectroscopy (XPS) and bremsstrahlung-excited Auger electron spectroscopy (AES) to characterize incipient oxide growth on commercially prepared Si_3N_4 powders as they are atmospherically oxidized at progressively higher temperatures up to 1200°C. Our analysis of the data emphasizes combined use of the Auger parameter and reference spectra to define the surface phases as the SiO_2 layer gradually thickens to obscure the substrate. The approach clearly isolates the beginning Si_3N_4 and final SiO_2 states throughout the course of the oxidation and gives no indication of an intermediate oxynitride phase for the powders under analysis. These results suggest that the Auger parameter method of analysis may have distinct advantages for determining the existence and identity of intermediate oxynitride phases on both superficially and heavily oxidized Si_3N_4.

II. EXPERIMENTAL

A. Sample Powders

Two commercially prepared Si_3N_4 powders, M-11 and SN-E10, were used as the starting materials in this study. The M-11 powder (H. C. Starck GmbH and Co., Newton, MA) had an average particle size of 0.63 μm and was made by direct nitridation

of silicon. The SN-E10 powder (Ube Industries, Ltd., Kogushi, Ube City, Japan) had an average particle size of 0.54 μm and was produced by reacting SiCl with NH_3 to form Si(NH) , which was then converted to Si_3N_4 . Bulk analysis of the materials showed approximately 1 wt. % of oxygen. Other bulk contaminants (Fe, Al, Ca) were detected at less than 700 ppm. Measurements with XPS showed that oxygen was the major surface impurity on the powders. The amount on the M-11 powder (10 at. %) was half as much as that found on the SNE-10 material. Fluorine was present on the surface of the M-11 powder at 3 at. %, while the concentration on the SN-E10 powder was ~10 times smaller. We attribute the larger F impurity on M-11 to a HF rinsing step used to clean the powders during processing.

During thermal oxidation the powders were placed in a 99.8 % alumina crucible and suspended in a thermogravimetric analyzer. The containment vessel was purged with He before heating to the oxidation temperature. Once the desired temperature was reached it was held there for 5 minutes before introducing the atmospheric oxidizing gas (ultra-high-purity N_2-20% O_2). The powders were oxidized for one hour at a given temperature over the range 700 - 1200 °C. After cooling to room temperature they were stored in clean glass containers. More detailed information on the material properties of the powders and their oxidation can be found in Ref. 1. A bulk Si_2N_2O powder (Norton Ceramics) was also included in the study to serve as a standard for the oxynitride bonding.

B. Surface Instrumentation

The surface composition and bonding of the Si_3N_4 powders were determined in an XPS mode using a multi-technique apparatus (Model 5600ci, Physical Electronics, Eden Prairie, MN). A dual anode x-ray source (Mg and Al) and a variable aperture hemispherical analyzer were the key instrumental components utilized in the analysis. The XPS data were obtained by irradiating the sample with $Mg_{K\alpha}$ x-rays ($h\nu$ = 1253.6 eV). It was possible to excite the Si KLL Auger transitions using the bremsstrahlung background from the source. Survey and high-resolution scans were obtained at pass energies of 23.50 and 187.85 eV, respectively. Spectrometer linearity and absolute energy positions were calibrated to give the Au $4f_{7/2}$, Ag $3d_{5/2}$, and Cu $2p_{3/2}$ peak positions within ± 0.10 eV of 84.00, 368.30, and 932.65 eV binding energy (BE) [8]. Measurements were made over a sample area of about 2 mm^2 on a coherent powder layer. The layer was formed on

indium foil using a double-sided pressing technique that revealed only surfaces internal to the parent powder.

C. Data Acquisition

Because the silicon nitride powders were electrically insulating, there was a pronounced charge shifting of the spectra (4.5 - 6.0 eV) relative to the Fermi level of the spectrometer. Nevertheless, it was possible to obtain reproducible, stable spectra using just the Mg x-ray source without a neutralizing flood gun. To be certain that the peak shapes and relative energy positions were unchanged over the observed range of charging, the effect of varying the source-to-sample distance was examined. The resultant differences in charging, as much as 2 eV, gave no other measurable changes in the spectra. As a precaution, in order to minimize the chance of experimental inconsistencies from charging, all the data were acquired using the same source-to-sample distance.

Freshly loaded powders exhibited a minimal carbon surface impurity as measured by the XPS. There was 1.5 - 2.5 at. % on the M-11 and about half as much on the SN-E10. The concentration increased slowly when the loaded powder layer was exposed to air. Because there were no other changes in the spectral content, a select number of samples were periodically used to check the spectrometer stability. The relative peak positions were always reproducible to $\pm$ 0.05 eV. The C 1s peak shape from the M-11 powders was characteristic of adventitious carbon [9] with a monotonically decreasing high energy tail. However, the C 1s peak shape from the SN-E10 powders was somewhat variable with a relatively large contribution sometimes appearing at binding energies above the principal peak position. When the C 1s spectra were referenced to adventitious carbon at 284.8 eV BE [8,9], the M-11 data gave the smoother trend in binding energy as a function of the oxidation. For this reason we have chosen to emphasize the M-11 data throughout the paper, even though the Auger parameter analysis gave the same overall results for the two powders.

III. RESULTS

A. Measurement of the Powder Oxidation with XPS and AES

The Si KLL, Si 2p, and N 1s XPS spectra obtained after oxidation of the M-11 powders are shown in Figs. 1 - 3 after carbon referencing. As the amount of surface oxygen increases with higher temperature the Si KLL peak shape shows a progressively stronger influence from a lower kinetic energy peak, which grows to dominate the spectrum after oxidation at 1200 °C (see Fig. 1). This high temperature peak is

attributable to a thick coating of SiO_2. As shown in Fig. 2, the Si 2p spectra are not as strongly affected by the oxidation. Only a single peak is resolved and the binding energy shifts from an initial value of 101.65 eV for Si_3N_4 to a value of 103.55 eV for SiO_2 after the oxidation at 1200 °C. Both the starting and final state binding energies agree well with reference values found in the literature [8]. The full-width-at-half-maximum (FWHM) of the Si 2p peak gradually increases from 1.84 to 2.43 eV with oxidation up to 1000 °C, before again narrowing to 1.85 eV at the highest temperature.

As shown in Fig. 3, the N 1s peak also increases in binding energy during the oxidation . A shift of 0.7 eV is found between 800 and 1000 ° C. However, in contrast to the Si 2p spectra the FWHM progressively decreases from 1.63 eV to 1.46 eV after the oxidation at 1100 °C, where the peak was last detected due to the thickening of the oxide layer. The O 1s peak (not shown) has a symmetrical, gauss-like shape similar to the N 1s and the FWHM decreases from 2.13 to 1.79 eV for the oxidation sequence. Its binding energy also increases in a manner similar to that for the N 1s transition. The F surface impurity, initially found at a value of 2.15 at. %, gradually decreases with temperature and is not detectable after the oxidation at 1200 °C.

Table 1 lists the XPS results for the oxidation of the M-11 powder. An equivalent set of data, obtained for the SNE-10 powder, gave the same trends as a function of oxidation. The large difference measured by XPS for the oxygen content of the two starting powders (a factor of two) narrowed to just a few percent as the oxidation progressed beyond 1000 °C. However, the Si KLL peaks revealed a larger disparity at the higher temperatures. The high kinetic energy Si KLL peak from the SNE-10 powder was attenuated 40 % more than that for the M-11 powder after oxidation at 1100 °C. These differences are undoubtedly due to the deeper penetration depth of the Si KLL electrons as compared to the lower kinetic energy electrons generated by the XPS. As a consequence, the Si KLL spectra are better able to distinguish differences in the thicker oxide layers found at the higher temperatures.

B. Analysis of the Silicon Oxidation States

In this section we describe how the endpoint reference spectra (Si_3N_4 and SiO_2) were combined with the Auger parameter to unambiguously define the Si surface states present during progressive oxidation of Si_3N_4. As originally proposed by Wagner [10] the Auger parameter, α, is a unique identifier of a given bonding state. It is calculated by measuring the difference between XPS and AES peaks and, consequently, is independent

of the shift in surface potential. Thus, α offers a distinct advantage for interpreting the present data set, where the electrically insulating powders charge under the x-ray source and lose their Fermi-level referencing. In analyzing the data we have used the endpoint reference spectra as the basis for simulating the Si KLL and Si 2p peak shapes, but have reinforced the chemical state content and internal consistency of the results by requiring that α link the XPS and AES data sets.

The endpoint reference spectra, Si_3N_4 and SiO_2, used in the simulations were taken from the M-11 starting powder and from a powder that had been oxidized at 1200 °C. The M-11 starting powder exhibited a native oxide (10 at. %) from air exposure after synthesis and the powder that was heavily oxidized at 1200 °C showed no traces of nitrogen in the XPS analysis. The SNE-10 starting powder was considered inappropriate as a reference because the oxide signal was much larger. As shown in Fig. 4, the peak shapes for the Si 2p and Si KLL reference spectra are practically identical for the two powder conditions. The two peaks seen in the reference Si KLL spectra are due to the KL_2L_2 (small) and KL_2L_3 (large) transitions. It is important to include the contribution from the KL_2L_2 peak in the Si_3N_4 simulation as it affects the overall peak shape in that region of the spectrum where the KL_2L_3 oxynitride and SiO_2 transitions appear. The endpoint spectra accurately and simply portray this aspect of the peak shape. The only noteworthy difference in the Si transitions for the two reference conditions is found on the high kinetic energy side of the large Si KLL peak, where the intensity from the starting powder has a relatively larger intensity than that from the fully oxidized material. Measurements by Okada et. al on Si_3N_4 powder [11], showing a similar Si KLL peak shape, have attributed such a high kinetic energy contribution to a nonstoichiometric nitride. For comparison the Si 2p and Si KLL peak shapes from a nonporous silica powder (Cab-O-Sil, Cabot Corporation) were nearly equivalent to those from the powder oxidized at 1200 °C, the only difference being that the FWHM was 0.3 eV larger for the Cab-O-Sil.

The M-11 starting powder represents a good, but less than ideal, choice as a reference for pure Si_3N_4 because it is covered with a native oxide. That portion of the Si that is bonded to the oxygen will add intensity to the high-binding (low-kinetic) energy side of the XPS (AES) peaks. If one chooses the Si 2p peak from SiO_2 as the most credible peak shape for a single bonding state, comparison with the reference Si_3N_4 peak

(shown in Fig. 4) reveals that the oxygen-related extra intensity on the high binding energy side is only 4 % of the total peak area. Also, as seen in Fig. 4, there was no measurable difference in the Si KLL profiles in the low kinetic energy region of the main peak where the native oxide produces a spectral contribution. The smaller effect produced by the native oxide on the Si KLL transition is anticipated due to the decreased surface sensitivity of the higher kinetic energy Auger electrons. The reference spectra were used in the simulations without background subtraction, as it was considered a potential source of peak shape inconsistency. This was of particular concern for the Si KLL peaks where the subtraction is required over a relatively large energy range.

We have calculated α as the sum of the Si 2p binding energy and the Si KLL kinetic energy, or the difference in kinetic energy between these two peaks plus the incident x-ray energy ($h\nu = 1253.6$ eV). This definition, where the x-ray energy is added to the difference, has been called the modified Auger parameter [10]. Even though α is independent of sample charging, reliable use of it as a chemical state identifier requires that the surface exhibit a uniform charging potential (minimal differential charging effects) to permit clear interpretation of the spectral features. This is the case for the current data set as no changes were found in the peak shapes when the surface potential was intentionally varied. The values of α for the Si_3N_4 and SiO_2 endpoint reference spectra were 1714.40 and 1712.35 eV, respectively [8].

Our analysis of the Si KLL and Si 2p data using the endpoint reference spectra and Auger parameter is best illustrated in connection with the M-11 powder that had been oxidized for one hour at 1000 °C. The Si KLL peak shape obtained after the oxidation at 1000 °C shows a contribution from two dominant Si bonding states that could be associated with the Si_3N_4 substrate, the final SiO_2 coating, or an oxynitride. As mentioned previously, the corresponding Si 2p peak only shows a broadening after oxidation at this temperature. Our analysis of the bonding states responsible for these spectra begins with a simulation of the Si KLL peak using a combination of reference peaks. As shown in Fig. 5, the peak can be fully simulated by appropriate scaling of just the two reference spectra for Si_3N_4 and SiO_2 with a separation of 3.15 eV. The peaks are located at 1612.10 and 1608.95, respectively. At this stage of the analysis the chief issue is determining the identity of the two contributing surface states. One can reasonably anticipate that, due to the aggressive oxidation environment, the lower kinetic energy peak is produced by SiO_2 .

The larger uncertainty appears to be identification of the second peak and whether it is due to the substrate or an oxynitride.

At this juncture the Auger parameter was invoked to link the chemical state content of the Si KLL peak with that of the Si 2p transition. The process involves using α to locate the energy positions of the states in the Si 2p peak based on their placement in the simulation of the Si KLL transition. For example, the location of the presumed SiO_2 state in the Si 2p energy region is found by subtracting the Si KLL peak position at 1612.10 eV from the value of α previously determined for SiO_2 (= 1712.35 eV). The same was done for the second peak under the assumption that it was Si_3N_4 with an α of 1714.40 eV. These energy positions determine the placement of the Si 2p reference spectra for the assumed chemical states. The reference peak intensities were then scaled to give a best fit to the experimental peak shape. In the course of this curvefitting the reference peak placements were allowed to vary $\pm$ 0.05 eV to take into account uncertainties in α. Within these restraints the Si 2p spectrum obtained at 1000 °C could be fully simulated by using only Si_3N_4 and SiO_2 component states (see Fig.6). The two simulation peaks were separated by 1.05 eV with binding energy values of 102.35 and 103.40 eV, respectively. Note that the binding energy for the Si_3N_4 has increased 0.70 eV relative to the carbon-referenced value for the starting powder. As such it could easily be confused with an intermediate oxynitride state.

Similar analyses were performed on the Si KLL and Si 2p spectra obtained on the samples oxidized at 800 and 900 °C. The simulations progressed in a manner identical to that found for the 1000 °C data. Only the endpoint reference spectra were needed to obtain good fits to the Si KLL and Si 2p spectra, although their relative contributions varied as a function of the oxygen concentration. The separation of the two basis peaks used to simulate the Si KLL spectra was 3.15 eV, the same value found in the simulation of the 1000 °C data. Because of the lower oxygen content, the simulation parameters were less clearly defined for the 800 °C data. For this case the Si KLL peak separation of 3.15 eV was centered over a 0.3 eV range of acceptable values, which was solely determined by the location of the SiO_2 contribution. The Si KLL spectrum for the M-11 oxidation at 1100 °C could not be simulated as well as the lower temperature data with the 3.15 eV reference peak separation. It was necessary to increase the separation to 3.30 eV to get a good fit. The dominant oxide peak at the lower kinetic energy was completely accounted for by the SiO_2 reference peak. The larger separation is not compatible with an oxynitride state, as

such an intermediate Si-O-N bonding configuration would have a smaller peak separation from the dominant oxide contribution (see next section). All the simulations were of a quality comparable to that for the spectra shown in Figs. 5 and 6. A summary of the simulation peak energies for the M-11 powder is found in Table 2.

The analysis of the SNE-10 powders was entirely consistent with these results. As mentioned earlier the SNE-10 always exhibited a thicker oxide than did the M-11 powder for the various oxidation treatments. Consequently, the simulation of the Si KLL peak from the SNE-10 powder after oxidation at 1100 °C represents analysis of the thickest oxide in this study. The results, in terms of the curvefitting, were of the same quality as found for the other simulations. However, in order to obtain a comparable fit for the Si KLL peak found after oxidation at 1100 °C it was necessary to use an even larger reference peak separation (3.45 eV) than was required for the same oxidation of the M-11 powder. For this oxidation condition there was an insignificant contribution to the Si 2p peak from the substrate. Thus, it was not possible to test the Auger parameter placement of this component to determine whether the Si 2p - Si KLL separation was equivalent to the other oxidized powders, thereby suggesting a change in sample potential as a function of depth into the material.

We have estimated the average thickness of the SiO_2 layer for a given oxidation temperature using the ratio of the Si_3N_4 to SiO_2 reference peak intensities that contributed to the Si KLL simulation. As has been shown by Wang et al. in their study of Si_3N_4 oxidation [6], this ratio (R_A) can be related to the average oxide thickness, z, on a flat surface by

$$R_A = D_N\lambda_{NN} / D_O\lambda_{OO} [e^{-z/\lambda_{NO}} / (1 - e^{-z/\lambda_{OO}})] \qquad (1)$$

where D_N and D_O are the volume densities of Si in Si_3N_4 and SiO_2 , respectively, and λ_{NO} ($= \lambda_{OO}$) is the attenuation length of the Si KLL electron in the SiO_2 layer. In that work Eq. 1 was modified to include the effect produced on the effective oxide thickness by a spherical particle shape, assuming the oxide thickness is much smaller than the particle radius. The resulting average oxide thickness, $d = (\pi / 2) z$, is then given by

$$d = -20.4 \ln [R_A / (R_A + 1.71)] \qquad (2)$$

where D_N = 0.0736 moles Si per cm^3, D_O = 0.0383 moles Si per cm^3, λ_{NO} = 32.0 Å, and λ_{NN} = 28.4 Å [12]. Table 3 shows the values for R_A and the corresponding oxide thicknesses calculated from Eq. 2 for oxidation of the M-11 and SNE-10 powders from 800 to 1100 ° C. The oxide thickness for the oxidation at 1000 °C is 13 - 14 Å, whereas that for the 1100 °C treatment is about 45 and 60 Å for the M-11 and SNE-10 powders, respectively.

In summary, our analysis of the Si KLL and Si 2p peak shapes for thermal oxidation up to 1100 ° C shows no measurable evidence of an oxynitride interphase for oxide thicknesses up to 60 Å. Within the experimental limits of the data acquisition and simulation routine the spectra are dominated by contributions from the Si_3N_4 substrate and a gradually thickening layer of SiO_2.

C. Examination of the Bulk Oxynitride Powder

The Si_2N_2O powder was analyzed in a fashion identical to that used for the oxidized Si_3N_4 powders. As shown in Fig. 7, the Si KLL spectrum was overall quite similar in shape to the Si_3N_4 and SiO_2 reference peaks. However, the peak shape was somewhat broadened on the low kinetic energy side of the main feature in the region associated with bonding to oxygen. As might be anticipated from the preceding analysis, the Si 2p peak showed even less disparity from the Si 2p reference peaks for Si_3N_4 and SiO_2. The FWHM of the Si 2p, O 1s, and N 1s peaks for the oxynitride were quite close to the values found for the starting Si_3N_4 powders.

Figure 7 also shows a simulation of the Si KLL peak for the oxynitride, for which the Si_3N_4 and SiO_2 reference peaks were used as a basis. The two reference peaks were separated by 2.30 eV, a value that is 0.85 eV smaller than that required for simulation of the oxidized Si_3N_4 powders. This is consistent with the trend expected for an intermediate phase material, such as Si_2N_2O, for which mixed nitrogen-oxygen coordination should produce an Si KLL transition located at a kinetic energy between that for the fully oxygen coordinated SiO_2 and the fully nitrogen coordinated Si_3N_4.

We have also determined the Auger parameter for the oxynitride and used it to verify the stoichiometry by applying an empirical formula developed by Rivière et al. [13].

The value of α obtained from the energy positions of the Si KLL and Si 2p peaks for the oxynitride is between 1713.95 and 1714.00 eV. Consistent with the charge transfer found in the mixed oxygen-nitrogen coordination, α for the oxynitride lies between the values found for Si_3N_4 and SiO_2, 1714.40 and 1712.35, respectively. Rivière et al. have examined the dependence of α on the oxygen-nitrogen ratio for a series of silicon oxynitride thin-film compositions. Their work gave the following relationship:

$$\alpha (x) = \alpha (Si_3N_4) - \Delta\alpha \{ 2x / [2x + 3n (1 - x)] \} \qquad (1)$$

where $x = O / (O + N)$, $\Delta\alpha = \alpha (Si_3N_4) - \alpha (SiO_2)$, and n is a constant that represents the relative contribution made by the oxygen and nitrogen to the extra-atomic relaxation of the silicon. We have used this equation to calculate $O / (O + N)$ for the bulk oxynitride powder of this study using the above range of values for α and $n = 4/3$, which is the average number determined by Rivière et al. This value of n corresponds to the nitrogen having a 30 % larger effect on the silicon than does the oxygen. For 1713.95 eV $< \alpha <$ 1714.00 eV, we get $0.56 > O / O + N > 0.48$, which translates to an oxynitride composition over the range $Si_2N_2O_{1.12}$ to $Si_2N_2O_{0.97}$. Consequently, the Auger parameter determination from the surface measurements is quite consistent with the known Si_2N_2O bulk composition.

IV. DISCUSSION

By making use of the Auger parameter to link the simulations of the Si KLL and Si 2p peak shapes it has been possible to clearly identify the Si surface states present during the incipient oxidation of Si_3N_4 powders. In the absence of this approach, particularly as it applies to the interpretation of the Si 2p spectra from carbon-referenced energy positions, it is possible to misinterpret the data by assigning an oxynitride to explain the Si 2p peak shape. The reason for this is the upward shift in binding energy that occurs in the carbon referencing as the incipient oxide begins to form and grow to a thickness of about 15 Å. Obviously, the carbon referencing is not equivalent for the superficial native oxide found on a air-exposed Si_3N_4 and for the distinct SiO_2 layer that is present after thermal oxidation.

Comparison of the Si peak positions listed in Table 2 for the M-11 powders shows that the shift in carbon referencing is between 0.65 and 0.70 eV. As a result the Si 2p binding energy for Si_3N_4 , initially found at 101.65 eV in good agreement with literature values, is displaced to 102.35 eV and out of the more commonly accepted reference range [8]. By the same argument the SiO_2 binding energy moves from 102.75 eV, relatively low versus the literature numbers, to a value of 103.40 eV. Realizing that the surface consists of only Si_3N_4 and SiO_2 , one sees the that the shift in charge referencing is also reflected by the N 1s and O 1s peak positions (see Tables 1 and 2). The consistency with the Si portion of the data, which used peak positions derived from the simulations, becomes apparent when the binding energy positions of the N 1s and Si 2p oxide peaks are plotted against each other, as shown in Fig. 8. There is a one-to-one correspondence for the two sets of numbers, a trend that further validates the simulation procedure. As indicated earlier the maximum uncertainty for this plot is the ± 0.15 eV error range associated with the oxide peak obtained for the oxidation at 800 °C. Even for this uncertainty the one-to-one correspondence for the reference shifting is still apparent. Note that the data do not progress continuously along the line as the oxidation temperature increases. This is an indication of the variability in the carbon referencing and is why a charge independent analysis of the spectra must be performed to rigorously define the chemical state composition. The same carbon-referencing behavior is found in connection with the SNE-10 powder, for which the shift is about 0.5 eV.

Du et al. [7] have found evidence that a distinct interphase oxynitride is formed when a Si_3N_4 thin film is thermally oxidized at 1300 °C. This treatment produced a much thicker oxide coating than was examined in the present study and it was necessary to remove the outermost SiO_2 coating by careful HF etching. Our results for oxide layers less than 60 Å in thickness show no evidence of an oxynitride. At some stage between the two sets of measurements there must be a point at which a detectable interphase begins to form. In this context the data taken for oxidation at 1100 ° C offer the best chance for such a determination because the oxide has become thick enough that the rate-limiting subsurface growth parameters may be in evidence at the oxide-substrate interface. The N 1s peak measured for this oxidation temperature can potentially give more information on the interphase region compared to the Si KLL Auger transition because it has a lower kinetic energy (smaller inelastic mean free path). Thus, the content of the N 1s peak is more heavily weighted to the region of the sample near the internal SiO_2 interface. Our XPS data

show that the N 1s peak shape is unchanged, with the exception of a some narrowing as the oxidation temperature is increased. This invariance plus the coincident energy shift versus the Si oxide states (found in Fig. 8) also supports the absence of the oxynitride. In contrast the measurements of Wang et al. [6] on the air oxidation of Si_3N_4 powders revealed a small high binding energy contribution to the N 1s peak, which was ascribed to an oxynitride state. That particular sample, oxidized at 1000 °C for several hours, exhibited an oxide thickness of only 22 Å, or less than half the thickest oxide film analyzed in this study.

We have tested the uniqueness of the simulations done for the oxidation at 1000 and 1100 °C by introducing a third state in the curvefitting that was located 2.3 eV higher in kinetic energy than the SiO_2 reference state. This would correspond to the position of an oxynitride with the composition of the Si_2N_2O bulk powder examined in this work. In doing this we held the endpoint reference states near the values already described in the preceding sections and increased the contribution of the oxynitride component until an unavoidable discrepancy was seen with the measured Si KLL peak shape. The departure occurred when the additional peak reached an intensity that was several percent of the total Si KLL peak area. This is a rough estimate of our ability to detect the oxynitride interphase with the current simulation technique. Within these limits we find no evidence of an oxynitride phase for either the M-11 or SNE-10 powders.

The shift of the carbon referenced states as a function of oxidation can be explained by the onset of band bending as the electronic structure of the thickening incipient oxide becomes more like SiO_2 [14]. Prior to the thermal oxidation the adventitious carbon is coupled to the Fermi level through the surface electronic states of the Si_3N_4 with its native oxide. As the oxidation progresses the carbon referencing is accomplished through the surface states in SiO_2 . It is the energy shift of the core states relative to the carbon referencing at the Fermi level, due to band bending between the Si_3N_4 and SiO_2, that gives the observed increase in binding energy as the oxide layer is formed. The XPS and AES measurements only analyze that portion of the Si_3N_4 that is subject to band bending near the interface with the SiO_2 . As shown in Fig. 9, the band bending can be explained by the band gap properties of the Si_3N_4 substrate ($E_g = 5.0$ eV) and the SiO_2 surface layer ($E_g =$ 9.0 eV) [15]. For insulating Si_3N_4 and SiO_2 with no surface or defect states, the Fermi level for both materials is nominally located at the mid-point of the band gap and a band

bending of 2.0 eV results if the materials are joined together. In order to explain the 0.7 eV shift seen in the M-11 data, we postulate a Si_3N_4 donor state that places the Fermi level 3.8 eV above the valence band, or 1.3 eV above the mid-point of the 5.0 eV-wide gap (see Fig. 9). Assuming that the Fermi level for the SiO_2 is at the mid-point of the band gap, this placement will explain the experimentally observed shift. This model is by no means unique, as any assignment of Fermi-level locations in the two materials that preserves this band bending will explain the data. Further information on the band-gap states is necessary to define the exact Fermi-level placements. The resultant band bending is equivalent to saying that the surface potential becomes more positive and, thus, after carbon referencing the binding energies are seen to increase. The band-bending adjustment occurs gradually as the oxide layer thickens and becomes more like bulk SiO_2 above 800 °C. For oxidation up to 800 °C the carbon is referenced to the Si_3N_4 Fermi level as the electronic structure of the SiO_2 is insufficient to produce the band bending. Because it is exceptionally thin, we suspect that the incipient oxide layer formed below 800 °C exhibits defects in stoichiometry and morphology, the latter perhaps from oxide nucleation. Because the band-gap states could vary from one material to another, perhaps due to impurity content, we anticipate that the oxidation of other Si_3N_4 materials may not exhibit the same referencing shifts, although the values obtained for the two materials of this study are quite similar.

A number of studies have used brehmsstrahung-excited Si KLL spectra to analyze Si-O-N bonding on Si_3N_4 powders [6,11,16-19] and thin films [20,21]. In addition to examining oxygen reactivity with these materials, the method has been used to analyze the nitridation of Si [19] and the effect of ion bombardment on the nitride bonding [20]. The obvious advantage in using the Auger transition is the larger energy separation between the Si_3N_4 and SiO_2 peaks as compared to that for the XPS peaks. Simulations of complex Si KLL peak shapes have been successfully performed to identify a variety of Si bonding states that range from elemental Si to SiO_2, including nonstoichiometric nitride compounds [11,19-21]. In some instances the Auger parameter has been calculated from these data to further define the chemical state content. For example, the native oxide found on commercial powders has been characterized by calculating the Auger parameter after curvefitting simulation of the Si 2p and Si KLL peaks [11]. In a modification of this approach the present work has interactively used Auger parameters as part of the Si 2p and Si KLL simulation process to avoid reference shifting and charging artifacts in the determination of the bonding states. This concept of linking the Si KLL and Si 2p

simulations using in-situ defined reference Auger parameters has been shown to offer some advantages for understanding the data taken on silicon nitride materials.

V. SUMMARY

Surface measurements have been made on two commercially prepared Si_3N_4 powders after they were oxidized at temperatures between 700 and 1200 °C in a high purity N_2 - 20% O_2 gas environment. The chemical state composition of the surfaces was determined using the Auger parameters for the initial (Si_3N_4) and final (SiO_2) bonding states to link the data obtained on the Si 2p and Si KLL transitions. The analysis showed no evidence of an interphase oxynitride for oxide film thicknesses up to 60 Å, as the peaks could be consistently simulated using just Si_3N_4 and SiO_2 curvefitting components. The XPS and AES transitions from the Si, N, and O states were found to uniformly shift to higher binding energies during the early stages of oxide growth (up to 15 Å thick), an effect that is attributable to band bending at the oxide-nitride interface. The present study has shown that incorrect identification of an oxynitride state can result if this energy shift is not taken into account in carbon referenced spectra.

ACKNOWLEDGMENTS

The authors would like to express their thanks to R. K. Schulze of Los Alamos National Laboratory for helpful discussions and critical reading of the manuscript.

REFERENCES

[1]. D. P. Butt, D. Albert, and T. N. Taylor, J. Am. Ceram. Soc. **79**, 2809 (1996). See references therein for a listing of studies on Si_3N_4 oxidation.

[2]. L. U. J. Ogbuji, J. Am Ceram. Soc. **78**, 1272 (1995).

[3]. B. W. Sheldon, J. Am. Ceram. Soc. **79**, 2993 (1996).

[4]. M. N. Rahaman, Y. Boiteux, and L. C. De Jongue, Am. Ceram. Soc. Bull. **65**, 1171 (1986).

[5]. L. U. T. Ogbuji and D. T. Jayne, J. Electrochem. Soc. **140**, 759 (1993).

[6]. P. S. Wang, S. G. Malghan, and S. M. Hsu, J. Mater. Res. **8**, 3168 (1993).

[7]. H. Du, R. E. Tressler, K. E. Spear, and C. G. Pantano, J. Electrochem. Soc. **136**, 1527 (1989).

[8]. J. F. Moulder, W. F. Stickle, P. E. Sobol, and K. D. Bomben, *Handbook of*

X-ray Photoelectron Spectroscopy (Physical Electronics Division, Perkin-Elmer Corp., Eden Prairie, MN, 1992).

[9]. T. L. Barr and S. Seal, J. Vac. Sci. Technol. A **13**, 1239 (1995).

[10]. C. D. Wagner, L. H. Gale, and R. H. Raymond, Anal. Chem. **51**, 466 (1979).

[11]. K.Okada, K. Fukuyama, and Y. Kameshima, J. A. Ceram. Soc. **78**, 2021 (1995).

[12]. S. Tanuma, C. J. Powell, and D. R Penn, Surf. Interf. Anal. **17**, 927 (1991).

[13]. J. C. Rivière, J. A. A. Crossley, and B. A. Sexton, J. Appl. Phys. **64**, 4584 (1988).

[14]. W. F. Egelhoff, Surf. Sci. Rep. **6**, 253 (1987).

[15]. S. M. Sze, *Physics of Semiconductor Devices* (New York, Wiley, 1981).

[16]. I. Bertóti, G. Varsányi, G. Mink, T. Székely, J. Vaivads, T. Millers, and J. Grabis, Surf. Interf. Anal. **12**, 527 (1988).

[17]. P. S. Wang, S. M. Hsu, S. G. Malghan, and T. N. Wittberg, J. Mater. Sci. **26**, 3249 (1991).

[18]. P. S. Wang, S. G. Malghan, S. M. Hsu, and T. N. Wittberg, Surf. Interf. Anal. **21**, 155 (1994).

[19]. P. S. Wang and T. N. Wittberg, Surf. Interf. Anal. **24**, 95 (1996).

[20]. J. A. Taylor, Appl. Surf. Sci. **7**, 168 (1981).

[21]. R. Padmanbhan and N. C. Saha, J. Vac. Sci. Technol. A **6**, 2226 (1988).

FIGURE CAPTIONS

Figure 1 - - - Si KLL transitions from the M-11 powder after oxidation for one hour at the indicated temperatures. The energy scale has been charge corrected by carbon referencing.

Figure 2 - - - Si 2p transitions from the M-11 powder after oxidation for one hour at the indicated temperatures. The energy scale has been charge corrected by carbon referencing.

Figure 3 - - - N 1s transitions from the M-11 powder after oxidation for one hour at the indicated temperatures. The energy scale has been charge corrected by carbon referencing.

Figure 4 --- Top : Si 2p reference spectra from Si_3N_4 (solid line) and SiO_2 (dashed line). Bottom : Si KLL reference spectra from Si_3N_4 (solid line) and SiO_2 (dashed line). The energy axis has been arbitrarily shifted to line up the peak maxima.

Figure 5 --- Simulation of the Si KLL transition from the M-11 powder after oxidation at 1000 °C. The Si_3N_4 and SiO_2 component peaks are indicated, as well as the difference between the data and the simulation. The energy scale has been charge corrected by carbon referencing.

Figure 6 --- Simulation of the Si 2p transition from the M-11 powder after oxidation at 1000 °C. The Si_3N_4 and SiO_2 component peaks are indicated, as well as the difference between the data and the simulation. The energy scale has been charge corrected by carbon referencing.

Figure 7 --- Simulation of the Si KLL transition from the bulk Si_2N_2O powder. The Si_3N_4 and SiO_2 reference peaks are indicated, as well as the difference between the data and the simulation. The energy scale has been charge corrected by carbon referencing.

Figure 8 --- Carbon referenced peak positions from the M -11 powder for the N 1s and Si 2p oxide component after oxidation at the specified temperatures.

Figure 9 --- Schematic of the band gap region for Si_3N_4 and SiO_2. The band bending is illustrated for alignment of the Fermi level, E_F, from the two materials. CB = conduction band, VB = valence band, and E_g = the band gap.

Table 1 Summary of XPS data obtained from the M-11 powder as a function of oxidation temperature. The data have been charge corrected for the C 1s peak at 284.8 eV BE.

	Atom Fraction	Binding Energy (eV)	FWHM (eV)
Received			
Si 2p	39.6	101.65	1.84
O 1s	10.1	532.25	2.13
N 1s	44.9	397.40	1.63
C 1s	2.4	284.80	2.59
F 1s	3.0	686.40	2.15
700 °C			
Si 2p	38.9	101.60	1.86
O 1s	15.6	532.15	2.07
N 1s	41.1	397.30	1.61
C 1s	2.4	284.80	2.57
F 1s	2.0	686.50	2.19
800 °C			
Si 2p	39.4	101.65	1.93
O 1s	20.1	532.00	2.02
N 1s	27.4	397.30	1.60
C 1s	1.38	284.80	2.57
F 1s	1.62	686.55	2.12
900 °C			
Si 2p	38.0	102.20	2.11
O 1s	29.6	532.55	1.84
N 1s	29.9	397.80	1.50
C 1s	1.52	284.80	2.41
F 1s	0.9	687.20	1.94

Table 1 (continued)

	Atom Fraction	Binding Energy (eV)	FWHM (eV)
1000 °C			
Si 2p	36.2	102.70	2.43
O 1s	42.6	532.70	1.78
N 1s	19.2	398.00	1.47
C 1s	1.38	284.80	2.35
F 1s	0.6	687.40	1.73
1100 °C			
Si 2p	33.6	103.20	1.89
O 1s	61.9	532.55	1.74
N 1s	2.5	397.85	1.46
C 1s	1.6	284.80	2.54
F 1s	0.4	687.30	1.76
1200 °C			
Si 2p	31.3	103.55	1.85
O 1s	59.4	532.80	1.79
C 1s	9.4	284.80	2.14

Table 2 XPS and AES peak positions for the M-11 powders in the as-received condition and after one-hour thermal oxidation at the specified temperatures. Where applicable the Si peak positions were obtained from the values used in the simulations. The data have been charge corrected for the C 1s peak at 284.8 eV BE.

	As-received	800 °C	900 °C	1000 °C	1100 °C	1200 °C
Si KLL (nitride) *	1612.75	1612.75	1612.30	1612.10	1612.35	
Si KLL (oxide) *		1609.60	1609.15	1608.95	1609.05	1608.80
Si 2p (nitride) †	101.65	101.65	102.15	102.35	102.05	
Si 2p (oxide) †		102.75	103.20	103.40	103.25	103.55
N 1s †	397.40	397.30	397.80	398.00	397.85	

* = eV kinetic energy

† = eV binding energy

Table 3 Values of the Si_3N_4 - to - SiO_2 ratio, R_A , and the oxide thickness, d, as a function of oxidation temperature for the M-11 and SNE-10 powders.

	M-11		SNE-10	
	R_A	d (Å)	R_A	d (Å)
800 °C	16.40	2.0	6.91	4.5
900 °C	5.76	5.3	4.34	6.8
1000 °C	1.95	12.8	1.67	14.4
1100 °C	0.19	47.0	0.09	61.1

FIGURE 1 / TAYLOR

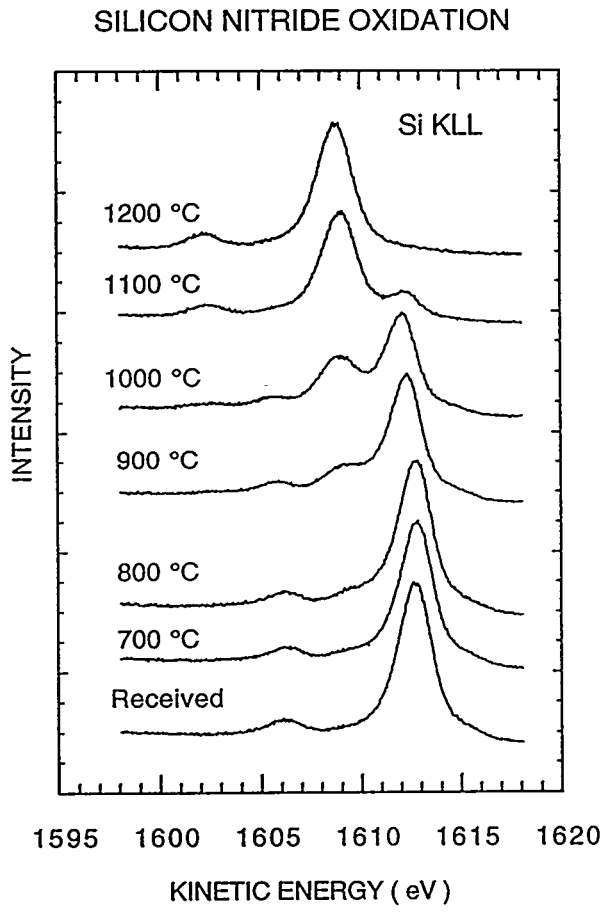

FIGURE 2 / TAYLOR

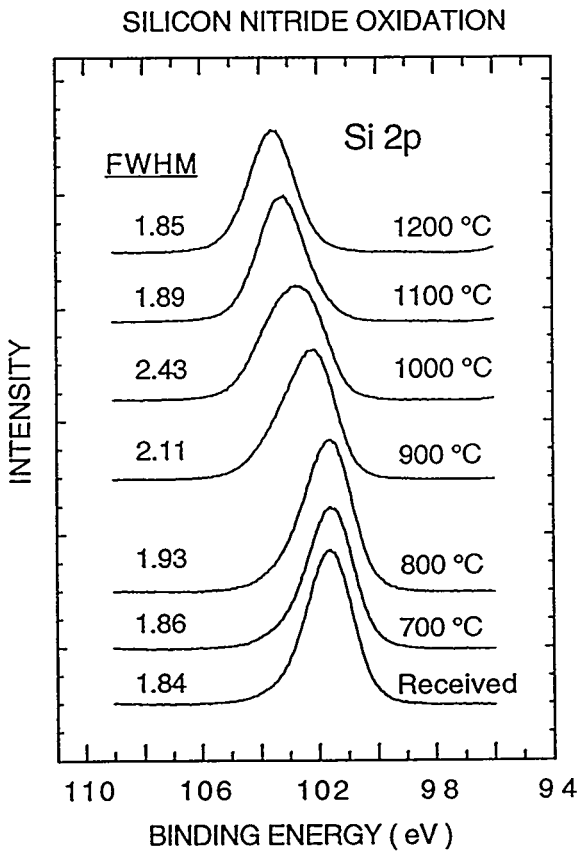

FIGURE 3 / TAYLOR

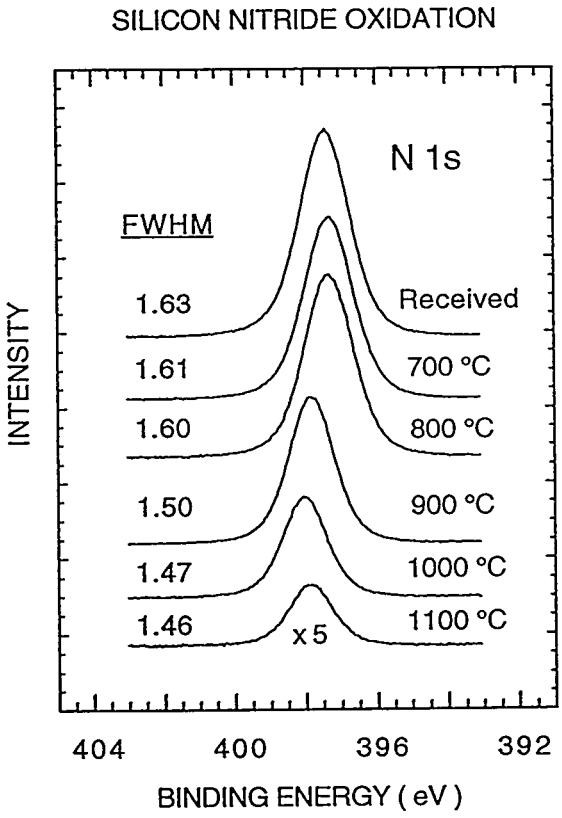

FIGURE 4 / TAYLOR

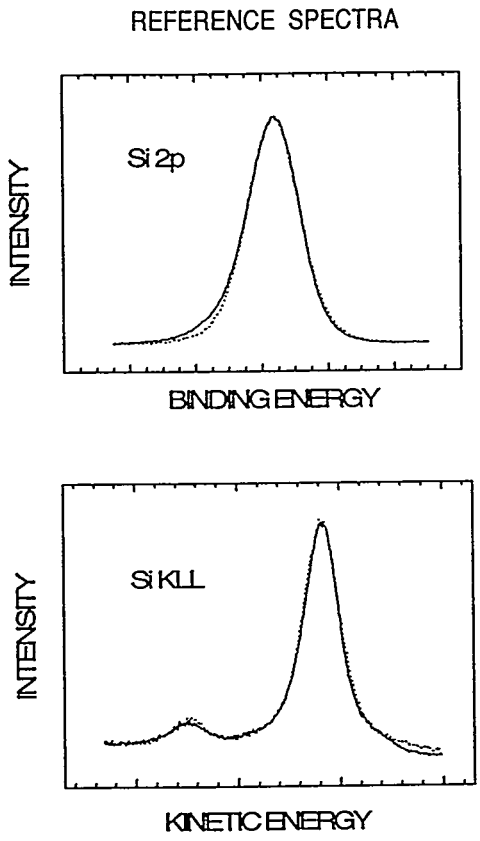

FIGURE 5 / TAYLOR

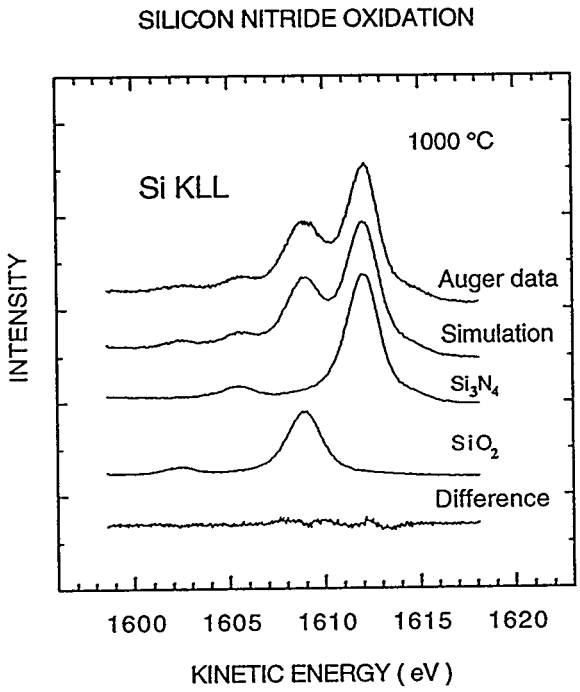

FIGURE 6 / TAYLOR

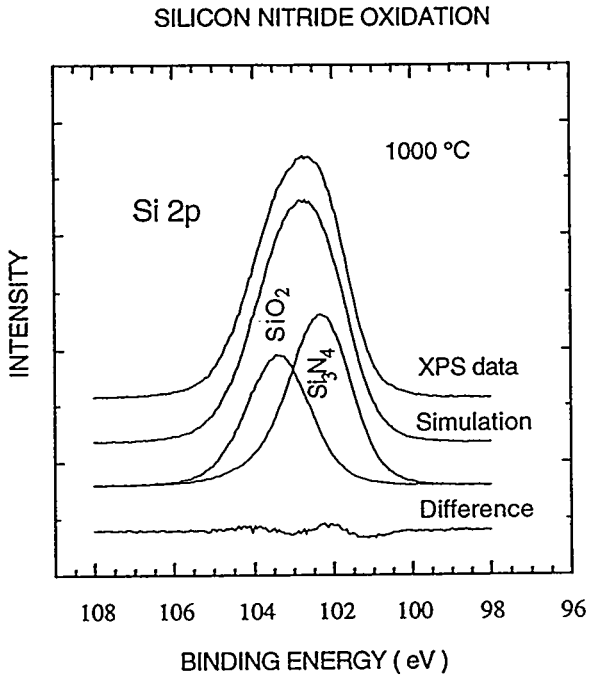

FIGURE 7 / TAYLOR

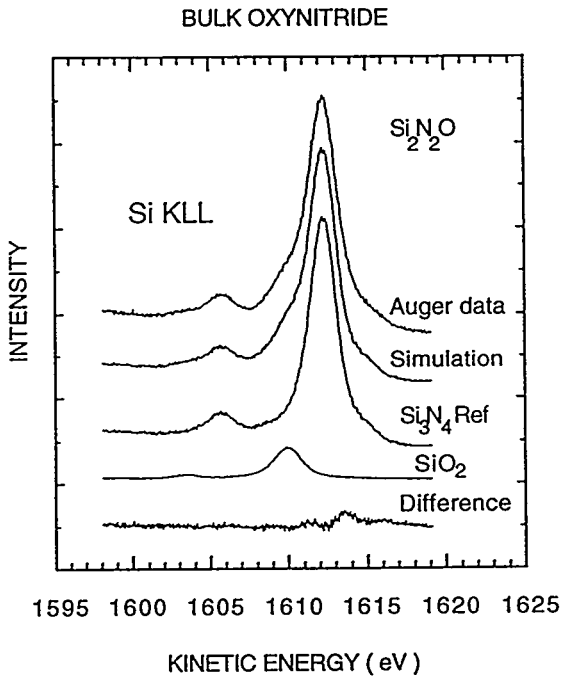

FIGURE 8 / TAYLOR

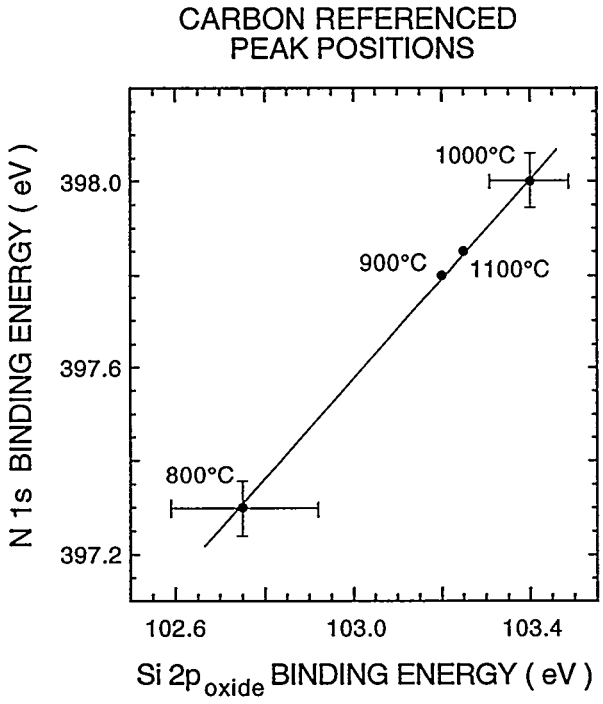

FIGURE 9 / TAYLOR